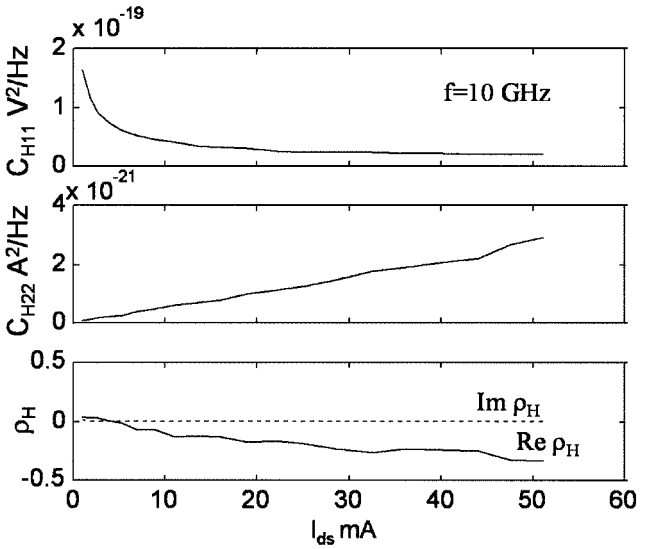

Figure 3 Drain-current dependence of hybrid correlation matrix C_H of a 0.5-μm gate-length conventional HEMT

results demonstrate that the real part of correlation coefficient at high-drain current is important. Experimental results up to 26 GHz using two different measurement methods confirm the simulations.

ACKNOWLEDGMENT

This work has been supported by Spanish Government under grants nos. TIC2000-0144-P4-02 and ESP2002-04141-C03-02 (MYCT), and a scholarship from CONACYT, Mexico.

REFERENCES

1. M.W. Pospieszalski, Modeling of noise parameters of MESFETs and MODFETs and their frequency and temperature dependence, IEEE Trans Microwave Theory Tech 37 9 (1989), 1340–1350.
2. R.A. Pucel, W. Struble, R. Hallgren, and U.L. Rohde, A general noise de-embedding procedure for packaged two-port linear active devices, IEEE Trans Microwave Theory Tech 40 (1992), 2013–2023.
3. H. Jong-Hee and K. Lee, A new extraction method for noise sources and correlation coefficient in MESFET, IEEE Trans Microwave Theory Tech 44 (1996), 487–492.
4. A. Lázaro, L. Pradell, and J.M. O'Callaghan, FET noise parameter determination using a novel technique based on 50Ω noise figure measurements, IEEE Trans Microwave Theory Tech 47 (1999), 315–324.
5. H. Happy, O. Pribetich, G. Dambrine, J. Alamkan, J. Cordier, and A. Cappy, HELENA: A new software for the design of MMICS, IEEE MTT-S Int Microwave Symp Dig 1991, pp. 627–630.
6. R. Singh, and C.M. Snowden, Small-signal characterisation of microwave and millimeter-wave HEMT's based on a physical model, IEEE Trans Microwave Theory Tech 44 (1996), 114–121.
7. F. Danneville, H. Happy, G. Dambrine, J. Belquin, and A. Cappy, Microscopic noise modelling and macroscopic noise models: How good a connection?, IEEE Trans Electron Dev 41 (1994), 779–785.
8. K.K. Thornber, Current equations for velocity overshoot, IEEE Electron Dev Lett 3 (1982), 69–71.
9. A. Lázaro, L. Pradell, and J.M. O'Callaghan, Novel method from measuring noise parameters of microwave two-port, IEE Electronics Lett 34 (1998), 1332–1333.
10. A. Lázaro, and L. Pradell, Extraction of the noise parameters of a transistor by using a spectrum analyser and 50Ω noise figure measurements only, IEE Electronic Lett 34 (1998), 2353–2354.

L-BAND ACTIVE RECEIVING ANTENNA FOR AUTOMOTIVE APPLICATIONS

Victor Rabinovich
Tenatronics Ltd.
Newmarket, Ontario,
Canada

Received 25 April 2003

ABSTRACT: *This paper describes L-band active receiving antenna for the automotive applications (DAB radio). The antenna is based on a printed dipole in 1452-1492 MHz frequency range and has a low noise amplifier. Two different versions of the antenna are presented: one for "on-vehicle" application (roof or trunk) and the second one for "in-vehicle" application (glass window). Antenna directionality is measured for on-vehicle and in-vehicle antenna locations.* © 2003 Wiley Periodicals, Inc. Microwave Opt Technol Lett 39: 319–323, 2003; Published online in Wiley InterScience (www.interscience.wiley.com). DOI 10.1002/mop.11203

Key words: *active antenna; low-noise amplifier; printed dipole; DAB radio*

1. INTRODUCTION

Microwave antennas integrated with the active elements—or active antennas—have received wide interest in mobile communications [1–4]. These antennas have the advantages of low cost, low profile, and light weight. This paper concerns two different versions of an active antenna for digital audio broadcasting radio (DAB) in the L-band frequency range. One of these active antennas can be used for "on-vehicle applications" and another one can be used for "in-vehicle" applications.

It is known that antenna pattern performances are very specific to the vehicle antenna location [5–7]. Reflections and shadowing effects can significantly change the antenna pattern. In contrast to the simulated results of the antenna on an ideal circular ground plane, only measurements of the antenna on the exact mounting location on the vehicle can show the real antenna performance. Therefore, a variety of measurements performed to study those effects in the DAB frequency band are presented in this paper.

2. ACTIVE ANTENNA SYSTEM DESIGN

As an antenna element, a printed on a thin dielectric substrate monopole is used. A surface-mounted low-profile omnidirectional monopoles are one of the popular types of antennas with vertical polarization performance [8–12]. The proposed antennas are fabricated on a cheap RF material FR-4 substrate with $\varepsilon_r = 4.5$. The substrate thickness is 1.6 mm. Figures 1 and 2 show two different antenna proposals. The first quarter wavelength antenna shown in Figure 1 is preferable for "on-vehicle" applications. Such an antenna can be used as the roof or trunk antenna. The second proposal, the bow-tie-shaped antenna shown in Figure 2 is preferable for "in-vehicle" applications. This antenna can be attached to the glass window. Extended ground in Figure 2 is used for 50Ω impedance matching. For the antenna shown in Figure 1, the amplifier circuit is arranged on the bottom side of the ground plane. According to Figure 2, the antenna patch and amplifier are placed on one side of a substrate, while the ground plane with extended ground parts is arranged on the other side of the substrate. The second antenna was designed and optimized for the L-band frequency range by using FEKO electromagnetic simulator [13]. Figures 3 and 4 show the measured input impedance and VSWR for these antennas without amplifiers.

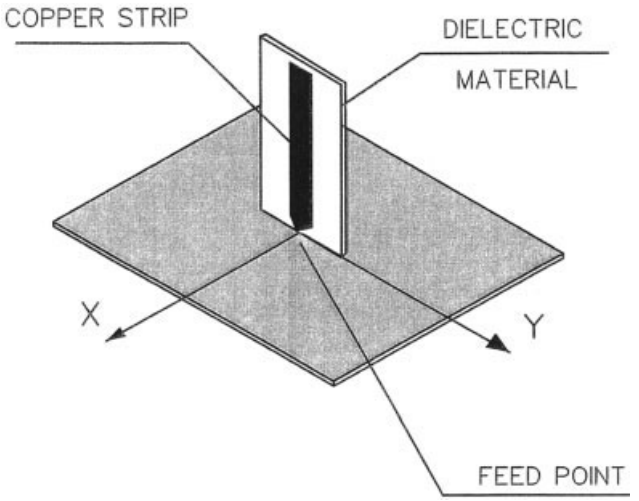

Figure 1 Geometry of the quarter wave antenna

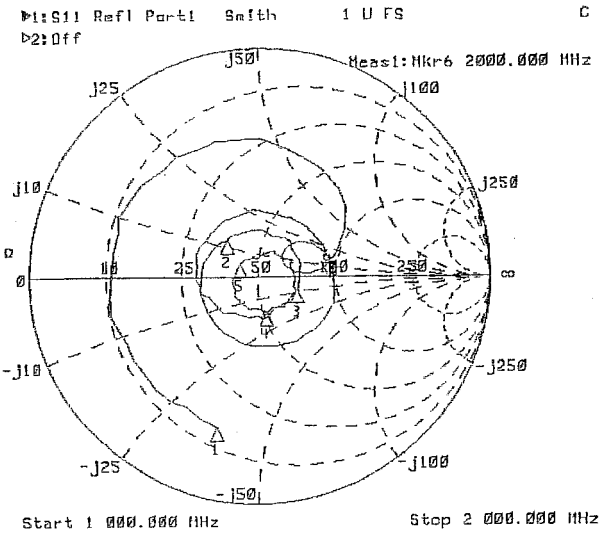

The amplifiers for both antennas were designed using computer software by Genesys [14]. Each amplifier has two transistor stages and a dielectric L-band filter. Both transistors are ATF 34143 from Agilent Technology and the dielectric L-band filter is from the TOKO company. Power gain of the amplifier in the L-band frequency band as a function of frequency is shown in Figure 5. The noise figure of the designed amplifier is about 1.3 dB. Noise-figure measurements were made with the aid of N8973A noise figure meter from Agilent Technology. The measured noise figure does not include losses of the monopole itself.

3. ANTENNA PATTERN MEASUREMENTS

The measurement site utilizes an automobile turntable (TENATRONICS Ltd. design) which can rotate the antenna itself (without a vehicle) or rotate the automobile with antenna to be measured. The turntable is placed on a hill to block outside reflections from any surrounding environment. The antenna-range instrumentation

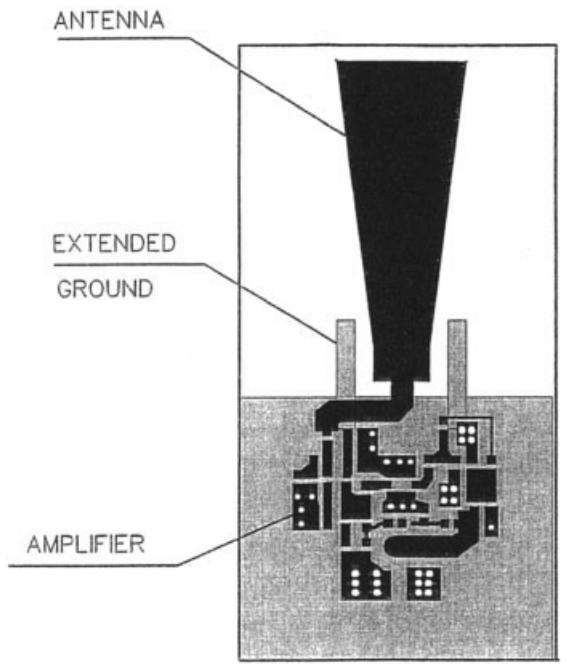

Figure 2 Geometry of the bow-tie-shaped antenna

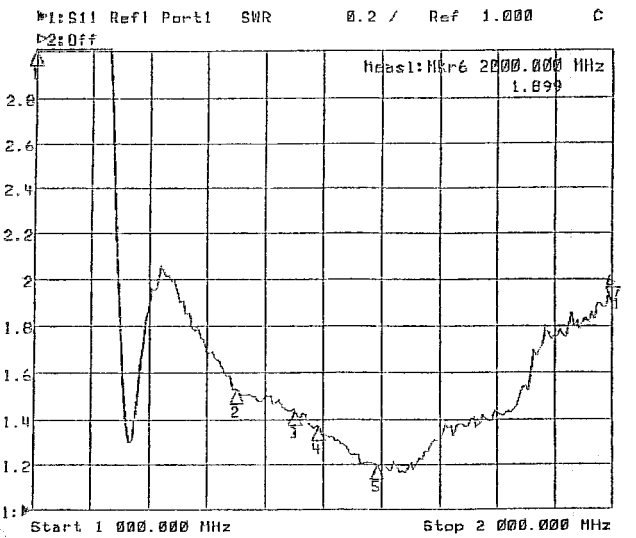

Figure 3 Smith chart and VSWR of the quarter-wave antenna on the metal plane

is controlled by a computer which drives the turntable rotation, controls a spectrum analyzer, and transfers measured data to the hard drive and printer. A data point was taken on the 0° elevation amplitude pattern every 2° as the turntable is rotated through a full 360° azimuth. For antenna measurements, we used a 2002 Pontiac Sunfire. Several tests for different vehicle antenna locations were performed.

4. ANTENNA PATTERN DATA ANALYSIS

1. Horizontal plane antenna patterns (without vehicle) measured in the automated anechoic chamber are omnidirectional. The gain of the first antenna on the metal plane with linear size $d/\lambda = 1$ (λ is the wavelength) is approximately the same as the gain of the wire monopole with the same

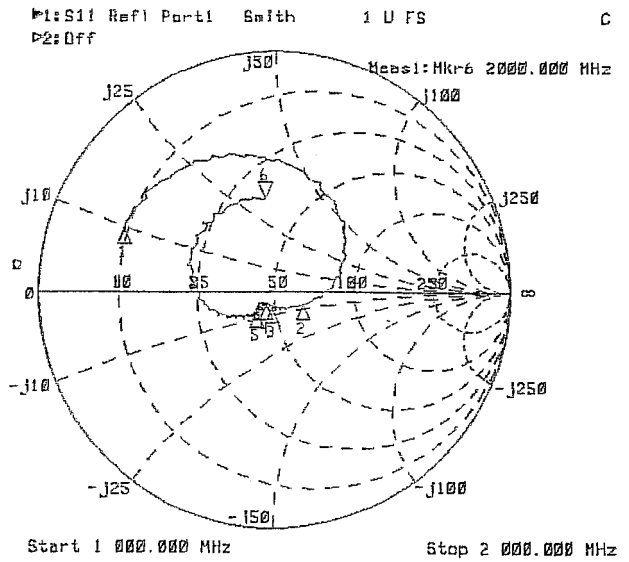

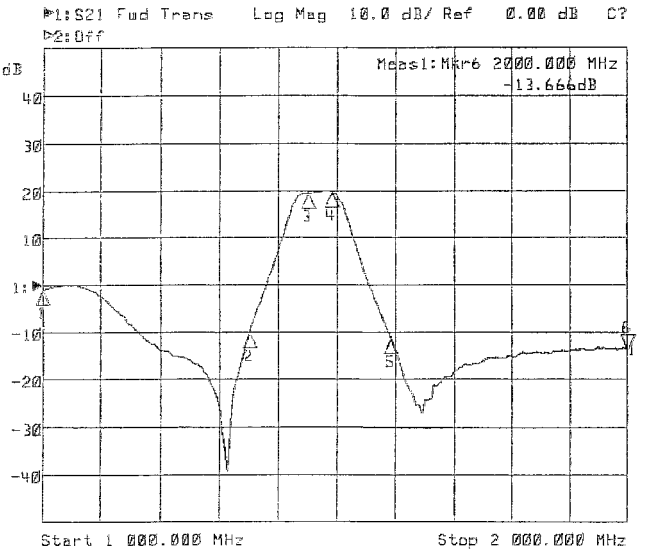

Figure 5 Amplifier gain

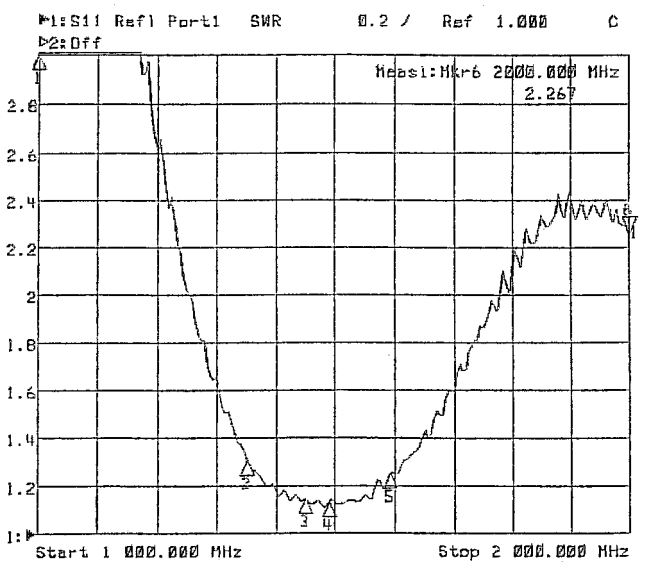

Figure 4 Smith chart and VSWR of the bow-tie-shaped antenna

ground plane. The gain of the second antenna is less than the gain of the free-space half-wave dipole by 0.5 dB.

2. Two "on-vehicle" antenna patterns measured on automobile turntable are shown in Figures 6 and 7. An angle direction of 270° on the charts is the direction of the front of the vehicle. The deviation of the omnidirectional pattern in Figure 6 is caused by the well-known [6] environmental influence of the vehicle. Figure 7 shows that the antenna placed on the trunk is becoming more directional. The average gain of over 360° for both antenna locations is the same. The deviation of an antenna pattern for the trunk-antenna location is more than the deviation for the roof antenna. The trunk-antenna location is reasonable if the roof is restricted or not available area for the antenna position. However, because roof and trunk antennas protrude from exterior surfaces of the vehicle, they are exposed to destructive impacts and create aerodynamic disturbances. For a convertible vehicle, the roof area is not available for antenna mounting. For this reason we investigated a few "in-vehicle" antenna positions.
3. Three "in-vehicle" antenna pattern are shown in Figures 8–10. The average gain of the side-glass antenna is less than the gain of the roof antenna by 2.7 dB; the average gains of the front- and back-glass antennas are less than the gain of the roof antenna by 6.5 dB. This low-gain level for the front- and back-glass window antennas can be explained by the inclined front- and back-window planes, compared to the vertical plane. Comparison of the three "in-vehicle" positions shows that the side-glass antenna location is preferable. Experimental results show significant directionality fluctuations of more than 360° for "in-vehicle" antenna positions. A space-diversity system [15] can be used to improve the reception from the "in-vehicle" antenna. This

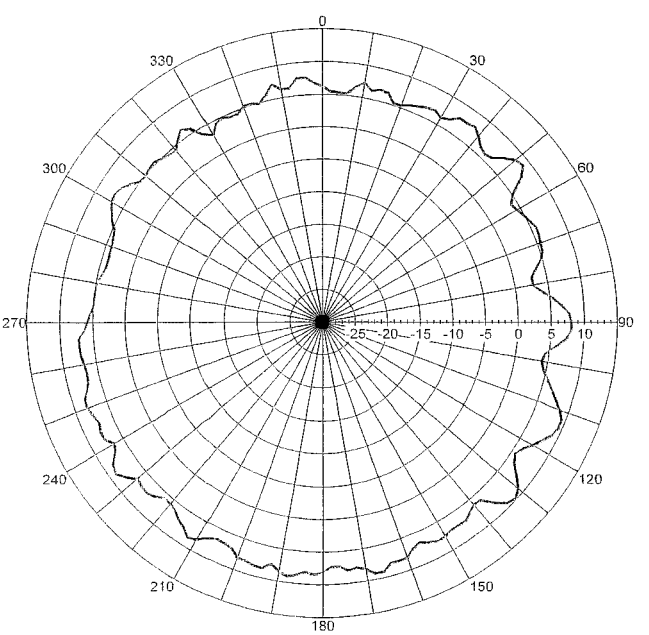

Figure 6 Radiation pattern of the roof-antenna location

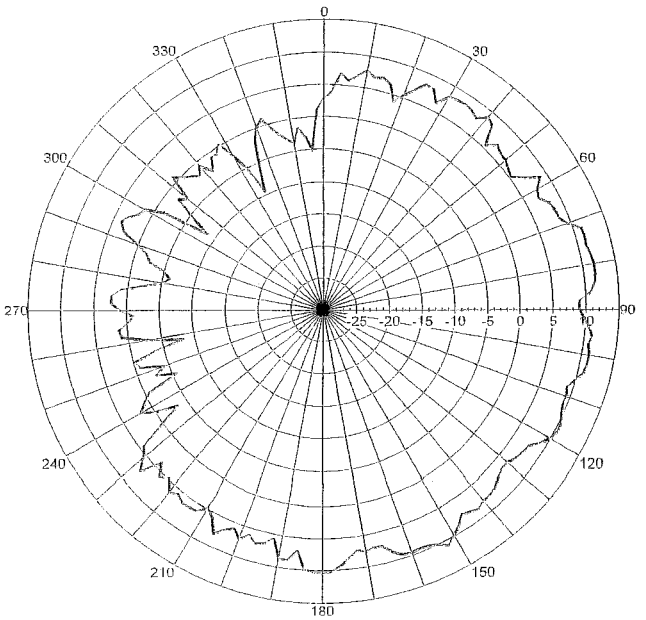

Figure 7 Radiation pattern of the trunk-antenna location

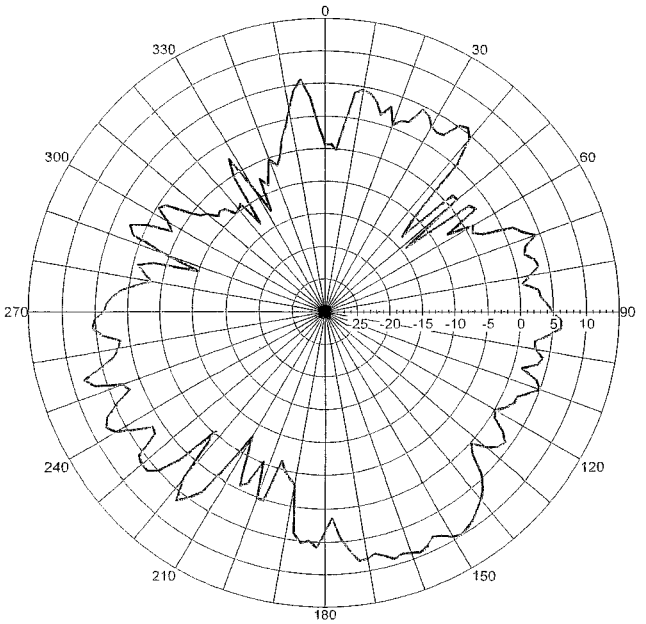

Figure 8 Radiation pattern of the antenna attached to the fixed side-glass window

technique requires two or more antennas. The greatest fading-reduction effect is expected when the correlation of the signals between the two antennas is near zero. The half-wavelength distance between the two antennas provides zero correlation in receiving signals [16] and improves the antenna system's performance.

5. CONCLUSION

We have been demonstrated that small-size flat monopole type active antennas can be used for L-band digital audio broadcasting application in the automotive industry. The "on-vehicle" and "in-vehicle" antenna patterns were measured using automobile turntable. The preferable locations of these antennas are investigated.

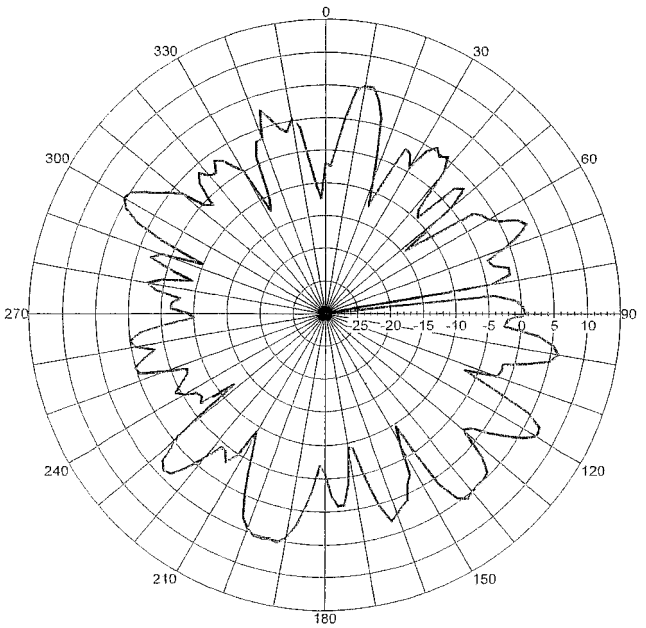

Figure 9 Radiation pattern of the antenna attached to the back-glass window

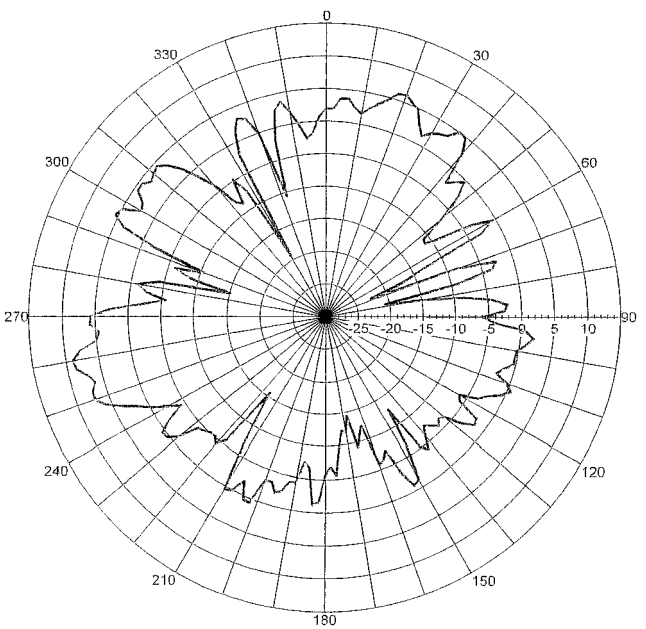

Figure 10 Radiation pattern of the antenna attached to the front-glass window

The proposed antennas can be used by themselves or in a space-diversity system.

REFERENCES

1. Y. Quian and T. Itoh, Progress in active integrated antennas and their applications, IEEE Trans Microwave Theory Tech 46 (1998), 1891–1900.
2. W. Duerr, W. Menzel, and H. Schumacher, A low-noise active receiving antenna using a SiGe HBT, IEEE Microwave Guided Wave Lett 7 (1997), 63–65.
3. V. Posadas, J. Martin, C. Frias, and C. Pascual, Development of high-efficiency active patch antennas, Microwave Opt Technol Lett 27 (2000), 122–125.

4. B. Robert, T. Razban, and A. Papiernik, Compact amplifier integration in square patch antenna, Electron Lett 28 (1992), 1808–1810.
5. C. Hill and T. Kneisel, Portable radio antenna performance in the 150, 450, 800, and 900 MHz Bands "Outside and In-Vehicle," IEEE Trans Vehic Technol 40 (1991), 750–756.
6. M. Daginnus, R. Kronberger, A. Stephan, J. Hopf, and H. Lindenmeier, SDARS antennas: Environmental influences, measurement, vehicle application investigations, and field experiences, SAE 2002 World Congress, Detroit, MI, 2002.
7. K. Fujimoto and J.R. James, Mobile antenna systems handbook, Artech House, Boston, 1994, pp. 336–337.
8. K.F. Tong, K.M. Luk, C.H. Chan, and E.N. Yung, A miniature monopole antenna for mobile communications, Microwave Opt Technol Lett 27 (2000), 262–263.
9. H.M. Chen, Microstrip-fed dual-frequency printed triangular monopole, Electron Lett 20 (2002), 619–620.
10. J. Lee, S. Park, and S. Lee, Bow-tie wide-band monopole antenna with the novel impedance-matching technique, Microwave Opt Technol Lett 33 (2002), 448–452.
11. H. Lebbar, M. Himdi, and J.P. Daniel, Analysis and size reduction of various printed monopoles with different shapes, Electron Lett 30 (1994), 1725–1726.
12. Y.-H. Suh and K. Chang, Low-cost microstrip-fed dual frequency printed dipole antenna for wireless communications, Electron Lett 36 (2000), 1177–1179.
13. FEKO Comprehensive EM Solutions, product of EMSS-SA (Pty) Ltd., Technopark, Stellenbocsh, South Africa, www.feko.co.za.
14. EAGLEWARE, RF and Microwave Design software, Eagleware Corporation, www.eagleware.com.
15. W.C.Y. Lee, Mobile communications engineering, McGraw-Hill, New York, 1982.
16. J.D. Parsons, The mobile radio propagation channel, Wiley, New York, 1996, pp. 137–140.

RELATIONSHIP BETWEEN ROOT-MEAN-SQUARE AND PEAK-TO-PEAK JITTER MEASUREMENTS

Dubravko Babić[1] and John Plombon[2]
[1] Etanvie Technologies
P.O. Box 60861
Palo Alto, CA 94306
[2] Intel Corporation
8674 Thornton Avenue
Newark, CA 94560

Received 21 April 2003

ABSTRACT: *The statistical relationship between peak-to-peak and root-mean-square (RMS) measurements of random and deterministic jitter is discussed. An analytic expression relating the two quantities is derived for normally distributed random jitter. This work is applicable to a production test of electronic or optical components that uses sampling oscilloscopes for jitter characterization.* © 2003 Wiley Periodicals, Inc. Microwave Opt Technol Lett 39: 323–326, 2003; Published online in Wiley InterScience (www.interscience.wiley.com). DOI 10.1002/mop.11204

Key words: *jitter measurement; random and deterministic jitter*

INTRODUCTION

Jitter is the fluctuation in the timing of a particular feature in the signal with respect to a reference clock. The conventionally observed feature is the crossing of the signal-transition edge with the decision level in the receiving chain. Jitter is a random variable described by its probability-density function (PDF) and its power-spectral density. These two functions are independent for stationary random variables and this case is generally present in optical and electronic systems. A communication system's ability to transmit information with better-than-specified bit-error ratio is tested and confirmed using "jitter test patterns" described in numerous standards [1–3]. Commercial tools exist that generate these test patterns and characterize the system response to the same patterns. However, in production-test environments, the characterization of jitter with fewer parameters and simple equipment is given preference due to cost and speed. Modern sampling oscilloscopes comprise the primary equipment in such test systems. They typically have built-in functions that quantify the measured waveforms. Two parameters used to characterize jitter that are of interest for this work are the root-mean-square (RMS), expressed as standard deviation (square-root of fluctuation variance) σ, and the peak-to-peak jitter value.

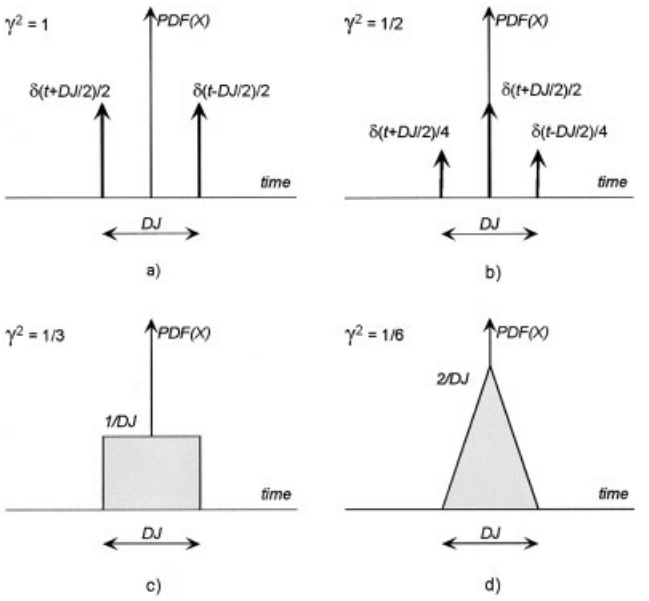

Figure 1 Four examples of simple bound jitter distributions. The peak-to-peak value for all distributions is equal to *DJ*

JITTER MODEL

It is widely accepted in the industry [1] that jitter encountered in electronic and optical sources can be measured with reasonable accuracy, and treated and specified as being a sum of one bound and one unbound jitter component. The unbound component originates from system noises (thermal, shot noise, and so on) and is referred to as random jitter. Random jitter is almost invariably assumed to be normally distributed. The bound component originates from various deterministic disturbances, such as signal or power supply crosstalk and intersymbol interference, and is commonly referred to as deterministic jitter. The essential feature of the deterministic-jitter distribution is that abruptly vanishes beyond certain jitter amplitude (see examples in Fig. 1). Although the shape of the deterministic-jitter distribution varies, the most widely used approximate PDF shape involves two δ functions [1]. These two components of jitter can be assumed to be independent random variables and hence the PDF of their sum is a convolution of the PDFs of each of the components [4]:

$$J(t) = \int D(t')\,R(t - t')dt', \qquad (1)$$